Optimization of a Graphene Nanoribbon through Eigenfrequency Analysis

M. van Ieperen (4386779), A. Zwemer (4451236), B. de Klerk, (4435168) and B. van Koppen (4443500)
Delft University of Technology, Faculty of 3mE, Precision and Microsystem Engineering - Group B4

***Abstract*— The world is getting bigger while devices are getting smaller. Accelerometers are no exception. This paper considers the optimization of a singly clamped - simply supported graphene-based accelerometer. We adapt and optimize existing theory on doubly clamped graphene membranes and build a macroscopic model to find a relation between the tension in the membrane and the corresponding eigenfrequencies. The macromodel allows us to gain more information about the singly clamped configuration, i.e. the behaviour of graphene membranes. The most intriguing finding is the wrinkling and rippling behaviour, resulting in a lower fundamental eigenfrequency of the membrane.**

***Keywords*— Accelerometer, Graphene, GNEMS, GNR, Eigenfrequency**

I. Introduction

Accelerometers have become a key instrument in our everyday life. From airbag deployment in automobiles to directional information in smartphones, accelerometers are an irreplaceable tool in many different industries. In current smartphones, the difference in electrical capacity due to inertia is measured with several comb drives to determine an acceleration. The size of these electromechanical devices are in the magnitude of millimeters [1]. Using graphene, a material with outstanding mechanical, electrical, thermal and optical properties, accelerometers can be scaled down to the microscale. These devices are called graphene nanoelectromechanical systems (GNEMS). An accelerometer with increased sensitivity can be achieved with a suspended graphene nanoribbon (GNR) [2]. Graphene can be exfoliated from graphite in which Van der Waals forces hold together the different layers of graphene. This single layer of carbon atoms is so thin that it can be considered as a two-dimensional membrane with great resonant characteristics. Not only does graphene have a Young's modulus of about 1 TPa and can it be stretched up to 20% without breaking, the resonance frequency of graphene can be measured electrically, which promises direct integration in electrical circuits making it the ideal material for a resonant accelerometer [3].

A suspended mass is directly connected to the GNR in an accelerometer. When this mass is subjected to an acceleration, the tension in the ribbon will change. The in- or decrease in tension gives a shift in the eigenfrequency of the membrane which can be measured in order to determine the acceleration. The eigenfrequency is the frequency where graphene takes on one of the mode shapes, i.e. the first mode shape is the fundamental mode. Besides the tension in the membrane, the eigenfrequency is also dependent on the geometric parameters of the GNR. The goal of this paper is to optimize the GNR for accelerometers by looking at a singly clamped configuration, instead of a doubly clamped membrane on which previous research is mostly based. The advantage of a singly clamped graphene membrane is that the mass can be chosen freely to change the tension in the membrane, calibrating it for a certain frequency range. This differs from using the inertia of graphene itself to change the tension in the membrane in a doubly clamped configuration.

Relatively low accelerations that will give large eigenfrequency shifts, applicable for sensitive accelerometers, are the main focus of this research. In order to do so, the different parameters which determine the resonance frequency are studied. Subsequently, a macroscopic model is built and compared to the simulation from COMSOL Multiphysics®.

II. Theory

A singly clamped beam with the other end simply supported is considered, as previously mentioned. For a resonator under tension T, the fundamental eigenfrequency f, is given by Eq. 1 [4], [5].

$$f = A\sqrt{\frac{Et^2}{\rho L^4} + \frac{T}{3.4 m_e L}} \tag{1}$$

The clamping coefficient, denoted by A, is 0.7085 for a singly clamped beam with the other end simply supported [6]. E is the Young's modulus, L is the length of the beam, ρ is the density of the material, t is the thickness, which is twice the Van der Waals radius of carbon [7]. m_e is the effective mass, which is a fraction of the mass of graphene: m_e = 0.5492m for a singly clamped beam. Eq. 1 is compared with a COMSOL model to check if it is accurate. Although they are not exactly the same, the formula is accurate within five percent, hence it is a good estimation.

The standard equation for the natural frequency, indicated with Eq. 2, can be combined with Eq. 1 which results in Eq. 3,

$$f = \frac{1}{2\pi}\sqrt{\frac{k_e}{m_e}} \tag{2}$$

$$k_e = 10.88\frac{Ewt^3}{L^3} + 5.83\frac{T}{L} \tag{3}$$

where the k_e is the effective spring constant and w is the width of the beam. The spring constant is essential because it can be used for scaling the microscopic to the macroscopic model. This will be thoroughly explained in the next section.

A. Optimization Theory of the GNR

In order to optimize the performance of the GNR, the frequency shift must be maximized so that the corresponding force as a consequence of the acceleration can be measured more accurately. Following from the equation for the frequency of the membrane, Eq. 1, the derivative of frequency over force is introduced, stated by Eq. 4.

$$\frac{df}{dT} = \frac{A}{6.8Lm_e\sqrt{\frac{Et^2}{\rho L^4} + \frac{T}{3.4m_eL}}} \tag{4}$$

The optimal situation is where there is a maximal frequency shift (df) for a change in force (dT). This results in a maximum value for df/dT, which realizes a more sensitive accelerometer. To do so, certain conditions have to be introduced. Firstly, the maximum measurable frequency of a graphene sheet with the setup available in the group of Prof. Steeneken is 250 MHz which is an upper limit for the frequency in the optimization. Secondly, there is a minimum width in order to support the force applied to the membrane. The corresponding relation is $T_{max} = \sigma_{UTS}wt$, where σ_{UTS} represents the ultimate tensile strength. This means that as the applied force increases, the width has to be larger to make sure the ultimate tensile strength is not surpassed, as illustrated in Fig. 1.

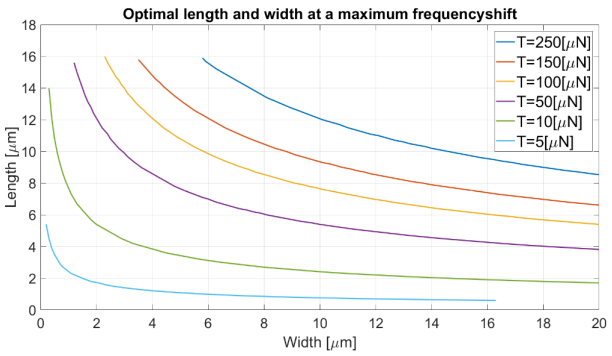

Fig. 1: The maximized derivative of the frequency over force while the frequency does not exceed 250 MHz and the width is large enough to carry the force. The optimal length and width for different applied forces on the GNR are indicated with coloured lines. Lower forces result in a higher df/dT, with values ranging from $5 \cdot 10^5$ - $12 \cdot 10^7$ MHz/N.

When the maximal value for the length (L_{max}) is chosen, it results in a minimal value for the width (w_{min}) and vice versa. Fig. 1 shows that the value for L_{max} is approximately 16 μm. This is verified when simplifying and filling in Eq. 1 with all the known values. L_{max} does not depend on the value of w_{min}, due to the fact the latter cancels out when T_{max} is inserted in Eq. 1. Since there is no relevant maximum value for the width, Fig. 1 is cut off at 20μm.

III. Experimentation

To compare the theory through simulations in COMSOL and calculations with experiments, a macroscopic model is fabricated. This is a simplified setup in the form of a single membrane that is easily measurable. The comparison of real test results and theory is most likely to show similar behaviour. In this case, the behaviour of the membrane is described by the spring constant as expressed in Eq. 3. The spring constant of the material, in the direction perpendicular to the membrane, has to remain constant when scaled from microscopic to macroscopic scale. The left part of Eq. 3 can be assumed negligible because $t \ll L$. This causes the effective spring constant to be only dependent on T and L.

A. Scaling

To gain appropriate geometric values for the macromodel, 55% of the ultimate tensile strength of graphene is used as the force. This percentage is chosen to be sure that the strain remains in the elastic region of elongation and such that $0.55\sigma_{UTS}wt \approx 50$ μN [8]. A GNR with a length of 12 μm and width of 2 μm is considered when scaling to the macromodel. These are geometric values picked from the optimum of 50 μN from Fig. 1. The dimensions of the macromodel are chosen so the spring constant and thus the behaviour will remain the same as for the micromodel [9]. The resonant frequency is also directly dependent on the tension in the membrane. The tension can be scaled up in the macroscopic setup. This way they should have the same mode shapes and show similar behaviour.

B. Setup

The setup for this experiment is displayed in Fig. 2. Using a PSV-400 Scanning Vibrometer®, the eigenfrequencies of different membranes subjected to various tensile loads are measured. Behind the membrane an exciter is mounted to a rectangular plate. This exciter generates a periodic chirp waveform with frequencies in the range of 0 - 500 Hz which are transferred to the membrane through air.

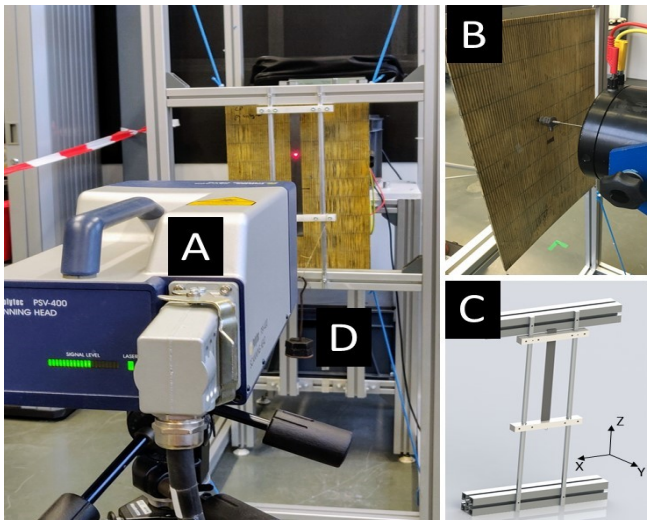

Fig. 2: The test setup. (**A**) The PSV-400 vibrometer. (**B**) The exciter with a plate attached to it. (**C**) The macromodel consisting of the suspended membrane. (**D**) The mass attached to the lower end exerting a force on the membrane.

Since it is impossible to use a graphene membrane for the macroscopic model, the material graphite was used

which consists of layers of graphene as mentioned earlier. The graphite membrane is suspended using 3D-printed clamps, the upper edge is fixed and the lower side can move only in the z-direction along the aluminum guide rails. The lower edge is subjected to various tensile loads using increasing weights.

C. Frequency Distortion

Since the lower edge of the graphite in the macromodel can move freely in the z-direction, it is necessary to investigate if the system encounters effects from the suspended mass. The suspended mass has an eigenfrequency, since it can move freely about the z-axis as well. When the eigenfrequencies of the graphite sheet and the mass overlap, this can result in distortion in the measured values. The mass is attached by two ropes which are connected at the lower clamp of the macromodel.

The spring constant of the ropes can be easily calculated, using the equation $k = AE/L$, where A is the cross section of the rope. The spring constant is circa $5.3 \cdot 10^5$ N/m for one rope.

IV. Results

The output of the vibrometer is the position-dependent displacement as a function of the actuation frequency. This results in a frequency range from 0-500 Hz with for each frequency the magnitude and corresponding modeshape displayed.

A. Frequency measurements

When only considering the fundamental mode shape, the frequencies of the macromodel can be plotted as a function of the force, see Fig. 3. The frequencies obtained by COMSOL are plotted as well, indicated with a dashed line. The 250x20 mm membrane, in Fig. 3 indicated with the blue line, has the same spring constant as the 12x2 μm graphene membrane from section III-A.

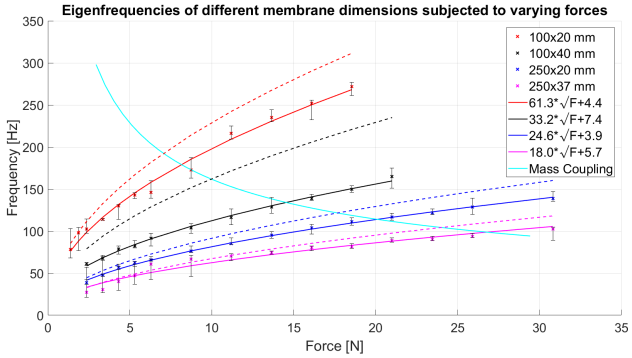

Fig. 3: The measured frequencies of the macromodel are indicated with dots, after which a square root line is fitted to these measurements with the curve fitting tool in Matlab®. The error bars are the random errors in the frequency measured. The frequencies that are obtained when using the same dimensions in COMSOL are plotted and indicated with a dashed line. The cyan line is the the calculated frequency of the mass-coupling

As expected from Eq. 1, the frequencies of the macromodel increase with a square root function of the force. The standard deviation for the 100x20 mm, 100x40 mm, 250x20 mm and 250x37 mm membranes with respect to the fitted lines are 6.5 Hz, 2.1 Hz, 0.9 Hz and 4.8 Hz respectively. It is clear that the frequencies of the macromodel are lower than the values obtained by COMSOL, but not with a constant difference.

B. Mass-coupling

With Eq. 2 the frequency as a function of mass can be plotted as is explained in section III-C. It unveils certain overlap in the eigenfrequencies. This happens close to the intersection of the mass coupling line with the experimental plotted lines of the membrane in Fig. 3. Besides that, the eigenfrequency of the GNR in the z-direction under the weight of the lower clamp is around 40 Hz. This results in higher errorbars at these frequencies.

The motions in the xz-plane and yz-plane are modeled as a pendulum with inertia. The frequencies derived from these calculations are approximately between 1 and 2 Hz and therefore have no influence on the eigenfrequency measurements of the graphite sheet.

C. Modeshapes

When observing the fundamental modeshapes in COMSOL, a different shape is displayed for the 100x40 mm membrane as depicted in Fig. 4. The larger the w/L ratio, the more the modeshape resembles Fig. 4(b) with respect to Fig. 4(a). In the 100x40 mm membrane of the macromodel this behaviour is not observed, as is depicted in Fig. 4(c).

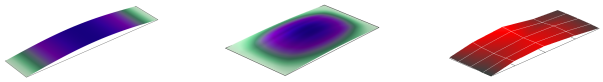

(a) 100x20 mm (b) 100x40 mm (c) 100x40 mm

Fig. 4: Fundamental modeshapes of graphite membranes with $E = 0.61$ GPa for the COMSOL model (a) & (b) and macromodel (c).

V. Discussion

As depicted in Fig. 3 the frequencies of the macromodel are smaller than the frequencies of the COMSOL model. Furthermore, the relative difference of frequencies between the macromodel and COMSOL model is not the same for every dimension. Both can be explained by several factors which are discussed in this section.

A. Rippling & Wrinkling

The fact that the frequencies calculated in COMSOL have larger values compared to the frequencies obtained from the macromodel can be justified by phenomena called rippling and wrinkling. The rippling and wrinkling results in wavelike shapes with certain heights. In free-standing graphene, *rippling* is caused due to thermal fluctuations and interatomic interactions that shapes the graphene sheet in the out-of-plane direction [10]. The graphite membrane from the macromodel is likely also prone to ripples. Static *wrinkling* is probably caused by uneven stresses near clamped edges of the membrane, accidentally produced during the fabrication of the macromodel [11]. The different dimensions which are tested may vary in the static wrinkling because some are clamped in with more uneven stresses than others.

The ripples and wrinkles could cause the effective length of the membrane to be longer than the geometric length. The geometric length is the shortest route from both clamping positions, thus having a straight path. The effective length follows the wave-like shapes caused by the ripples and wrinkles, hence being longer. An increased length gives a lower frequency as can be concluded from Eq. 1. This validates the results from Fig. 3.

B. Modeshapes

The modeshape behavior obtained by COMSOL that is depicted in Fig. 4(b) is not observed in the macromodel. This behaviour can be explained by the fact that the effective length is larger than the geometric length. This results in a smaller w/L ratio, and thus a behavior like Fig. 4(a). Another explanation of the difference in modeshapes is the way the force is simulated in COMSOL and in the macromodel. In COMSOL, a constant tensile force is exerted on one edge. In the macromodel, the force exerted by the mass is not constant during the measurements due to mass-coupling.

C. Friction

A possible error of the setup is that the force caused by the masses is not fully exerted on the membrane, but is partially exerted on the aluminum bars due to friction, resulting in a lower tension in the membrane and thus lower frequency. Therefore, the friction is a possible explanation for the difference between the macromodel and the COMSOL values.

D. Measurement Errors

1) Systematic Errors: Since the left part of Eq. 1 is negligible, the error in the Young's Modulus can be neglected. There are systematic errors which are constant for all measurements in all membranes, namely ρ, t, m_s and f, where m_s is the mass of the suspended load. There are also systematic errors that differ for different membranes, but are constant for all measurements, which are L and w. The standard deviations of these parameters are estimated by $\sigma_\rho = 40$ kg/m^3, $\sigma_t = 0.05$ μm, $\sigma_{m_s} = 0.5$ g, $\sigma_f = 0.3$ Hz, $\sigma_L = 1$ mm and $\sigma_w = 0.5$ mm, respectively. This results in a total maximum systematic error in the frequency of 2.4%. Defects in the material can cause a systematic error as well. These defects can emanate from the fabrication of the material.

2) Random Errors: The random error differ for each measurement and is caused by inaccuracy of the measured f. This error is on average much larger than the systematic errors. This error is depicted in Fig. 3 by the error bars. It is clear that this error can vary enormously. It is probable that the large random error is caused by noise during experimentation.

VI. Conclusion & Recommendations

The objective of this research was to design and optimize a graphene based accelerometer. This resulted in a singly clamped configuration of the GNR. Existing theory on doubly clamped membranes was studied, after which modified equations were obtained to determine the optimal geometric values of the graphene membrane for different tensile forces. From this it follows that L_{max} is around 16 μm for every value of w_{min}. Subsequently, using the results from the theory, a macroscopic model was designed and fabricated consisting of a graphite membrane in order to simulate the GNR. Various tensile loads were applied to the material, which resulted in the square root relation between force and frequency, corresponding to the theory. It is clear that the macromodel frequencies are significantly lower than the COMSOL model frequencies. This can be explained by various factors as discussed. The most promising factor is the intriguing behaviour of rippling and wrinkling, caused by interatomic interactions and thermal fluctuations in the material as well as uneven stresses at the clamping of the membrane. These phenomena could justify the difference in the comparison of the macromodel with the micromodel.

Recommended for further research is using the obtained results of the theory and translating this to the design of an actual accelerometer. Also, the effects of mass-coupling on the frequency measurements can be reduced by optimizing the macromodel design. This can be done by applying the force differently on the membrane. Lastly, the properties of rippling and wrinkling behaviour can be further examined, since this plays a significant role in the behaviour of the membrane. Finding the relation between the geometric and effective length would therefore be a recommendation for further research.

Acknowledgements

The authors thank G. Verbiest for his insights and for the support and help in understanding the theory involved. The authors thank R. van Ostayen for helping with simulations in COMSOL. Furthermore, the authors acknowledge support and discussion concerning the subject from R. van Ostayen, J.G. Buijnsters and S. Lampaert.

References

[1] A.M. Hurst, S. Lee, W. Cha, and J. Hone, "A Graphene Accelerometer," 2015.

[2] J.W. Kang et al., "Developing accelerometers based on graphene nanoribbon resonators," *Physics Letters*, vol. A 376, pp. 3248–3255, 2012.

[3] F.T. Shi, S.C. Fan, C. Li and X.B. Peng, "Modeling and analysis of a novel ultrasensitive differential resonant graphene micro-accelerometer with wide measurement range," *MDPI*, 2018.

[4] I.W. Frank, D.M. Tanenbaum, A.M. van der Zande and P.L. McEuen, "Mechanical properties of suspended graphene sheets," *American Vacuum Society*, vol. B 25(6), 2007.

[5] J. Scott Bunch et al., "Electromechanical resonators from graphene sheets," *Science*, vol. 315, pp. 490–493, 2007.

[6] S.M.Han, H. Benaroya, T. Wei, "Dynamics of transversely vibrating beams using four engineering theories," *Journal of Sound and Vibration*, vol. 225(5), pp. 935–988, 1999.

[7] Frank Weinhold, "Natural steric analysis: Ab initio van der Waals radii of atoms and ions," *Journal of Chemical Science*, 1997.

[8] M. Topsakal and S. Ciraci, "Elastic and plastic deformation of graphene, silicene, and boron nitride honeycomb nanoribbons under uniaxial tension: A first-principles density-functional theory study," *American Physical Society*, vol. 81, 2010.

[9] Andres Castellanos-Gomez, Vibhor Singh, Herre S.J. van der Zant, and Gary A. Steele, "Mechanics of freely-suspended ultrathin layered materials," pp. 12–14, 2014.

[10] Shikai Deng and Vikas Berry, "Wrinkled, rippled and crumpled graphene: an overview of formation mechanism, electronic properties, and applications," pp. 198–199, 2016.

[11] Ryan J.T. Nicholl et. al, "The effect of intrinsic crumpling on the mechanics of free-standing graphene," 2015.